Journal Homepage: http://ijcpe.uobaghdad.edu.iq
Iraqi Journal of Chemical and Petroleum Engineering
Vol. 26 No. 1 (March 2025) 23 – 34
EISSN: 2618-0707, PISSN: 1997-4884

Evaluation of microfiltration and ultrafiltration membranes for improving water quality: removal of turbidity, suspended solids, and bacteria from the Tigris River

Noor Jasim Al-Tamimi [a, *], Ahmed Faiq Al-Alawy [a], Muayad Al-Shaeli [b]

a Department of Chemical Engineering, College of Engineering, University of Baghdad, Baghdad, Iraq
b Paul Wurth Chair, Faculty of Science, Technology and Medicine, University of Luxembourg, Avenue de l'Universit'e, L-4365 Esch-sur-Alzette, Luxembourg

Abstract

The Tigris River in Baghdad is increasingly polluted by industrial and agricultural activities and untreated sewage, posing serious risks to public health and the environment. This pollution degrades water quality through various physical, chemical, and biological contaminants. This research aims to use membrane filtration techniques to treat Tigris River water, improving water quality and ensuring a clean, safe water supply. The study assesses the efficiency of polypropylene (P.P) 1µm, ceramic 0.5µm microfiltration, and polyvinylidene fluoride (PVDF) 500KD ultrafiltration membranes in removing turbidity, total suspended solids (TSS), and E. coli, and their impact on permeate flux. Experiments were conducted at a temperature of 25°C and a flow rate of 20 L/h, with regular intervals and an initial turbidity of 65 NTU. The results indicated that after 1.25 hours of operations, the permeate flux decreased by 23.12% for polypropylene membranes, 32.63% for ceramic membranes, and 38.48% for PVDF membranes. The PVDF membrane demonstrated the best performance, removing 98.7% of turbidity, 88% of total suspended solids (TSS), and 100% of E. coli. This makes it the most efficient membrane among the tested options. Hermia's model was used to study fouling in crossflow ultrafiltration (UF) and microfiltration (MF) membranes. Results showed that cake formation and standard pore-blocking models best predicted flux behavior for the ceramic membrane, while complete and intermediate pore-blocking models were more effective for the PVDF membrane. This study shows that membrane filtration improves Tigris River water quality by removing turbidity, suspended solids, and bacteria, ensuring a safe water supply.

Keywords: Microfiltration; Ultrafiltration; Tigris River; Hermia model; Membrane fouling.

Received on 21/10/2024, Received in Revised Form on 30/11/2024, Accepted on 30/11/2024, Published on 30/03/2025

https://doi.org/10.31699/IJCPE.2025.1.3

1- Introduction

Freshwater sources like rivers and lakes are crucial for maintaining a healthy society. Unfortunately, these resources have been consistently contaminated globally due to rapid development and flood hazard mitigation in recent decades [1]. Rivers serve as a critical water source globally, supplying human needs but also accumulating contamination from human sewage, oily and radioactive materials, organic and inorganic compounds, and biological pollutants. Lifestyle changes and population growth have intensely increased water demand and diversified its uses, making water quality a significant concern [2, 3]. According to the recommendations of the World Health Organization [4], regular monitoring and evaluation of water quality are essential. This needs frequent ecological, biological, and physicochemical assessments and examination of water supplies [5].

The Tigris River is one of the most important rivers in the world, which originates in southeastern Turkey, where its length is (1970 km) within the Iraqi borders, and the area of the river basin within the Iraqi borders is (2,166,155 km^2) [6]. The river's physical characteristics—such as temperature, turbidity, and hardness are valuable indicators of pollution levels. Additionally, chemical parameters like electrical conductivity, pH, and concentrations of ions (K^+, Na^+, Cl^-, and NO^{3-}) play an important role in identifying river water contamination [7]. Microbiological contamination further influences treatment requirements and the safe recycling of effluents in river waters [8].

In general, raw water can be filtered using deep sand-grain beds, granular organic carbon, membrane filtration, or a combination of methods [9]. When employing membrane filtration techniques such as microfiltration (MF), ultrafiltration (UF), nanofiltration (NF), and reverse osmosis (RO), the removal of bacteria, micro-organisms, particulate matter, small pollutants, and natural organic materials is effectively achieved [10, 11]. Microfiltration is typically utilized to remove bacteria, suspended particles, and substances with sizes ranging from 0.1 to 10 µm. On the other hand, ultrafiltration can separate particles between 0.001 and 0.1 µm, macromolecules, and colloids from water [12]. However, most of the dissolved ionic species still pass through the membrane [13].

*Corresponding Author: Email: Nour.Hammadi2207M@coeng.uobaghdad.edu.iq

In many applications, membrane processes compete directly with the more conventional techniques. However, compared to these conventional procedures membrane processes are often more energy-efficient [14], simpler to operate, and yield higher-quality products. Furthermore, the environmental impact of all membrane processes is relatively low [15]. There are no hazardous chemicals used in the processes that have to be discharged and there is no heat generation [16]. Despite their advantages, membrane processes face some limitations, especially in water and, wastewater treatment. One major issue is their susceptibility to fouling due to chemical interaction with water constituents, necessitating extensive pretreatment [17].

The variety of membrane separation processes differs in membrane type, configuration, transport mechanisms, and pore sizes, as well as process-driving forces [18]. Pressure-driven processes also vary in membrane pore size, allowing specific impurities to be selectively removed [19]. MF typically operates at low transmembrane pressures (1–2 bar) and serves as a pretreatment step for desalination techniques such as RO, NF, and electrodialysis [20], whereas UF requires pressures of 2-10 bar [21].

Microfiltration and ultrafiltration membranes are effective technologies for removing impurities and suspended particles [22]. However, these membranes are susceptible to fouling, which occurs when pollutants accumulate on or within the membrane, forming a gel layer that clogs the pores and reduces efficiency. Understanding the mechanisms of fouling and finding ways to mitigate its impact is essential for optimizing the performance of these filtration systems [23, 24]. Polymeric membranes, such as those made from hydrophobic polymers like polypropylene (PP) and polyvinylidene fluoride (PVDF), polyether sulfone (PES), polysulfide (PS) and polyacrylonitrile (PAN), are especially prone to fouling [25, 26] leading to decreased performance and increased operational costs due to required cleaning processes[27, 28]. Not all MF or UF membranes foul at the same rate, as differences in polymer composition and surface properties (e.g., hydrophobicity, roughness, pore size, geometry, and charge density) can affect the rate of foulant attachment [29]. Fouling mechanisms are driven mainly by the electrostatic and van der Waals interactions between colloidal particles and the membrane surface, as well as between the particles themselves [29]. Common fouling models include complete blocking, standard blocking, intermediate blocking, and cake filtration models [30]. Periodic membrane cleaning is required to remove pollutants and extend the membrane lifespan [31].

This study aims to treat Tigris River water in line with Iraqi drinking water standards, focusing on membrane filtration as an alternative to conventional methods. Specifically, ultrafiltration and microfiltration processes were evaluated for their effectiveness in removing turbidity, total suspended solids (TSS), and bacteria. Different membranes including hollow fiber PVDF UF, two MF membranes, P.P, and a ceramic were tested for their efficacy. Hermia's model was applied to analyze fouling mechanisms involved in cross-flow UF and MF membranes treating Tigris River water.

2- Hermia model

According to Darcy's law, the permeation flux of particle-free water across a clean membrane is as follows Eq. 1:

$$J = \frac{\Delta p}{\mu R_m} \quad (1)$$

Where J (m^3 m^{-2} s^{-1}) is the permeation flux, μ (kg/m. sec) is the absolute viscosity of the water, Δp (pa) is the Transmembrane pressure (TMP), and R_m (m^{-1}) is the clean membrane's hydraulic resistance.

In membrane filtration techniques, membrane fouling refers to different processes that reduce the efficiency of the membrane, leading to a decrease in permeation flux (the rate of fluid flow across the membrane) [32].

As a result, the permeation flux of MF, and UF units treating Tigris River water can be expressed, by modifying Eq. 2, as follows [33]:

$$J = \frac{\Delta p}{\mu(R_p + R_m + R_c)} \quad (2)$$

The resistance arising from cake formation is represented by R_c (m^{-1}), and the resistance due to pore blocking is represented by R_p (m^{-1}). In the beginning, both R_p and R_c are zero, so the initial permeate flux J_0 for microfiltration and ultrafiltration at a fixed TMP will mainly depend on Rm. Throughout the MF and UF processes, there can be a shift from membrane resistance to pore-blocking resistance or cake resistance. As the microfiltration operation progresses, pore blocking and cake formation will cause R_p and R_c to increase, altering the relative significance of R_m, R_p, and R_c in Eq 2. J_o is permeation flux at the beginning of filtration, so when $t = 0$, $J = J_o$ Based on this, four fouling mechanisms can be summarized [34]:

1. Complete blocking model

The complete blocking model assumes that particles arrive at the membrane and seal the membrane pores such that the particles are not superimposed upon each other. The blocked surface area is proportional to the permeate volume, as represented in Eq. 3.

$$J = J_0 \exp(-k_b t) \quad (3)$$

The equation can be simplified to Eq. 4.

$$\ln(J) = \ln(J_0) - k_b t \quad (4)$$

2. Standard blocking model

In the standard blocking model, the particle diameter is much less than the pore diameter, so, the particles can enter most pores, and deposit on the pore walls, thus

reducing the pore volume. The decrease of the pore volume is also proportional to the permeate volume, as represented in Eq. 5.

$$J = J_0\left(1+\frac{1}{2}k_s(AJ_0)^{0.5}t\right)^{-2} \quad (5)$$

At constant pressure, the term (AJ_o) is constant and the equation can be simplified to Eq. 6.

$$\left(\frac{1}{J^{0.5}}\right) = \left(\frac{1}{J_0^{0.5}}\right) + k_s t \quad (6)$$

3. Intermediate blocking model

In the intermediate blocking model, the number of blocked pores or surfaces is also assumed to be proportional to the permeate volume but, it is less restrictive in such a way that not every particle necessarily blocks the pores and particles may settle on other particles, as represented in Eq. 7.

$$J = J_0(1+k_i A J_0 t)^{-1} \quad (7)$$

At constant pressure, the term (AJ_o) is constant and the equation can be simplified to Eq. 8.

$$\left(\frac{1}{J}\right) = \left(\frac{1}{J_0}\right) + k_i t \quad (8)$$

4. The cake filtration model

The cake filtration model is used to explain the case of large particles, which cannot enter most pores, and hence, the deposit forms a cake on the membrane surface, as represented in Eq. 9.

$$J = J_0(1+2k_C(AJ_0)^2 t)^{-0.5} \quad (9)$$

The term (AJ_o) is constant at constant pressure, and the equation can be simplified to Eq. 10.

$$\left(\frac{1}{J^2}\right) = \left(\frac{1}{J_0^2}\right) + k_c t \quad (10)$$

Where J_o depends on the membrane resistance and transmembrane pressure, the viscosity of the permeate is expressed as follows: $J_o = \Delta P / \mu R_m$.

The various *K* terms represent mass transfer coefficients for the associated filtration laws [35]. Where $k_s = (1/2)k_s A^{0.5}$, $k_i = k_i A$, $k_C = 2k_C A^2$.

Specifically, to determine the most appropriate fouling model and obtain mass transport parameters, the flow functions on the left side of each model must be plotted against time. Specifically, plotting ln(*J*) vs. t, $(1/J^{0.5})$ vs. t, $(1/J)$ vs. t, and $(1/J^2)$ vs. t must be a straight line with a slope of k_b, k_s, k_i, and k_c, for complete pore blocking, standard pore blocking, intermediate pore blocking, and cake filtration models, respectively. The y-intercepts of these plots will be $\ln(J_0)$, $(1/J_0^{0.5})$, $(1/J_0)$, and $(1/J_0^2)$ respectively. The effectiveness and suitability of different fouling models can be evaluated by comparing the correlation coefficient values ($R^{2)}$ obtained from the linear regression analysis of these plots [36].

The size of membrane pores plays a crucial role in the fouling mechanism. When the size of the feed molecules is similar to the membrane pore size, partial clogging may occur. If the pores are larger than the feed molecules, particles can settle into the pores, leading to irreversible fouling. Conversely, if the pores are smaller than the molecules, these molecules accumulate on the membrane surface, potentially clogging the pores or forming a gel layer [37].

3- Experimental work

Real water samples were collected from the Tigris River at Adhamiya (Al-Masnaya) in mid-April 2024 to assess the efficiency of microfiltration (P.P 1 µm and ceramic 0.5 µm) and ultrafiltration (PVDF 500 KD) membranes on actual river water. Before the MF process, the pH of the raw water was measured using a pH meter (STARTER 2000, Switzerland). Turbidity was assessed with a turbidity meter (TB 300 IR), and temperature was recorded with a thermometer (model TM-902C, China). Total suspended solids were analyzed in the central general environment laboratory, while total coliform and E. coli levels were determined using the Most Probable Number (MPN) method. Specifications for the Tigris River feed water are presented in Table 1. The experiment evaluated permeate flux, turbidity, and membrane recovery for microfiltration and ultrafiltration membranes. Membrane characteristics are provided in Table 2.

Table 1. Feed water characteristics of the Tigris River in Baghdad during April month /2024

Temp °C	25 ±1°C
PH	7.88
E.C us/cm	628
TDS mg/l	310
TSS mg/l	39
Turbidity NTU	65
M.P.N of Total coli form /100 ml	2200
M.P. N of E. coli /100 ml	1700

Table 2. Specification of membranes used in this study

Specification	**P.P (MF)**	**Ceramic (MF)**	**PVDF (UF)**
material	Polypropylene	ZrO_2-TiO_2	Polyvinylidene fluoride
Pore size or MWCO	1µm	0.5µm	500KD
Membrane dimension	6.3 x 25cm	50 x 180mm	61x 325mm
Reaction to water	Hydrophobic	Hydrophilic	Hydrophobic
Working temperature	≤ 50 ºC	5 ºC- 80 ºC	5 ºC - 45 ºC
Way of filtration	in-to-outside	in-to-outside	in-to-outside
Membrane area	0.051 m^2	0.083 m^2	0.78 m^2
Working pressure	0-0.15 bar	0-0.15 bar	0-0.15 bar
PH range	0-12	0-12	2-13

Permeation flux (J) is the volume of permeate (V) collected per unit membrane area (A) per unit time (t), which is represented in Eq.11:

$$J = \frac{v}{A \cdot t} \quad (11)$$

The efficiency of removing turbidity can be calculated according to the Eq.12:

$$Re\% = \left(1 - \frac{Cp}{C_f}\right) \times 100\% \quad (12)$$

Where Re % is the turbidity removal efficiency, C_p is the permeate concentration in the water outlet stream (effluent) and C_f is the feed water concentration in the inlet water stream (influent).

The recovery represents the percentage of fee flow that crosses the membrane and turns into a permeate stream. It serves as a measure of the effectiveness of the membrane system by determining the ratio of the permeate volume to the feed, and can be calculated according to Eq.13:

$$R_w\% = \frac{Qp}{Q_F} \times 100\% \quad (13)$$

Where R_w is the recovery percentage Q_P is the permeate flow rate (product flow rate), and Q_F is the feed flow rate.

The experimental setup used in all the experiments is shown in Fig. 1. The setup operated in cross-flow mode and was designed to allow control of important operating parameters such as temperature, operating pressure, volumetric flow rate, and initial turbidity in the microfiltration (MF) and ultrafiltration (UF) processes. The initial turbidity of Tigris River water was 65 NTU. The system consisted of a 40 L plastic vessel with a stirrer (model OS20S, Shaanxi, China) to keep the feed concentration. The solution was withdrawn from the feed vessel via a diaphragm pump passed through a flowmeter set at 20 L/h, then through a pressure gauge to measure the operational pressure before being introduced to MF or UF membranes to remove turbidity, suspended solids, and certain types of bacteria. The permeate was collected every 15 min and its volume was measured and recorded using a digital balance. The concentrate was collected in another container, and the turbidity in the feed and permeate solutions were analyzed using a turbidity meter.

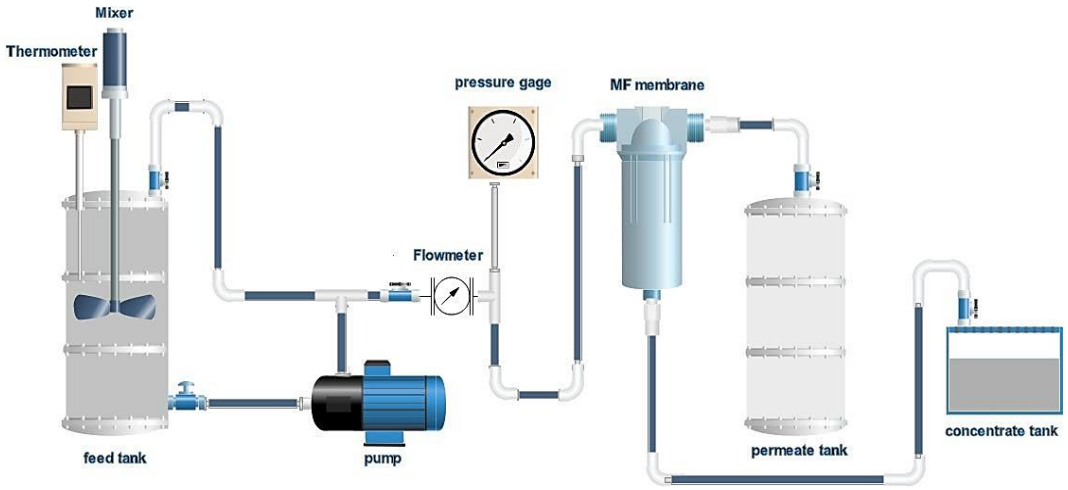

Fig. 1. Schematic diagram of the lab scale membrane system

4- Result and discussion

4.1. Permeation flux decline

Flux values and efficiency of the membranes can be influenced by operating parameters such as flow rate, temperature, turbidity concentration, membrane characteristics, and the materials they are made of [38]. The decline in MF and UF permeate flux for three membranes (P.P 1µm MF, ceramic 0.5µm MF, and PVDF 500KD UF) with time is shown in Fig. 2 to Fig. 4. The experiments were conducted under the same operating conditions: flow rate of 20 l/h, initial concentration 65 NTU, and temperature of 25°C. The flux of the polypropylene membrane decreased from 292.15 L/m^{2}h to 224.62 L/m^{2}h, from 326.42 L/m^{2}h to 219.89 L/m^{2}h for the ceramic membrane, and from 14.42 L/m^{2}h to 8.87 L/m^{2}h for PVDF membrane after 1.25 hours of operation. These results represent a decrease of 23.11% for polypropylene membranes, 32.63% for ceramic membranes, and 38.48% for PVDF membranes.

The total suspended solids (TSS) and turbidity on the membrane surface accumulation can gradually reduce permeate flux. The extent of this impact depends on membrane pore size and operational conditions. Over time, particles build up on the surface, forming a cake layer that can block pores and reduce flux. Variations in permeate flux among different membranes are primarily influenced by pore size, fouling sensitivity, and each membrane's physical and chemical properties. Membranes with smaller pores, such as PVDF and ceramics, experience a greater reduction in flux, as Tigris River water contains natural organic matter (NOM), which tends to adhere to the surface of finer membranes. Additionally, the surface properties of these membranes contribute to attracting and fixing molecules more than polypropylene membranes, which exhibit a smaller

decrease in flux due to their larger pores and enhanced resistance to fouling.

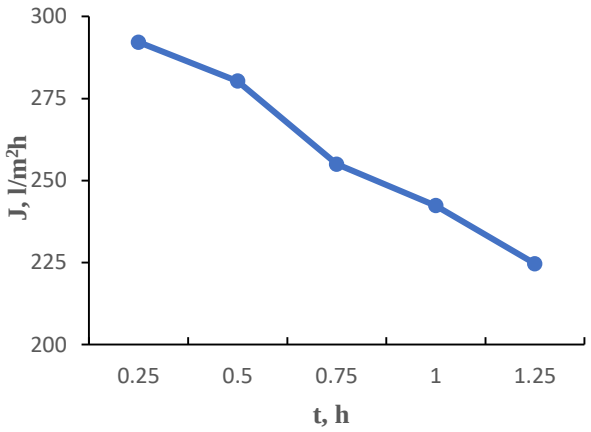

Fig. 2. Permeate flux declined over time for MF polypropylene membrane at Co=65 NTU, T=25°C, and QF=20 L/h

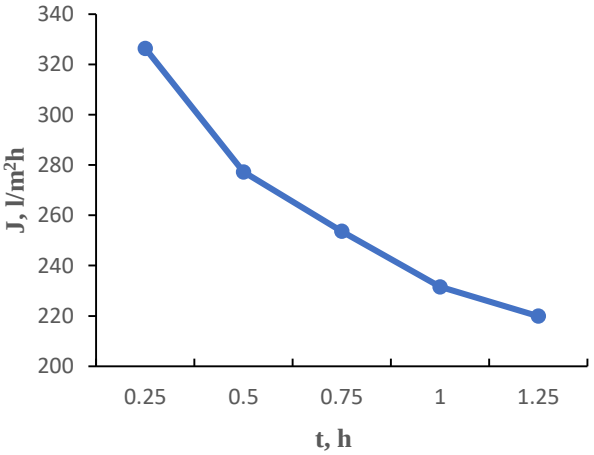

Fig. 3. Permeate flux declined over time for MF ceramic membrane at Co=65 NTU, T=25°C, and QF=20 L/h

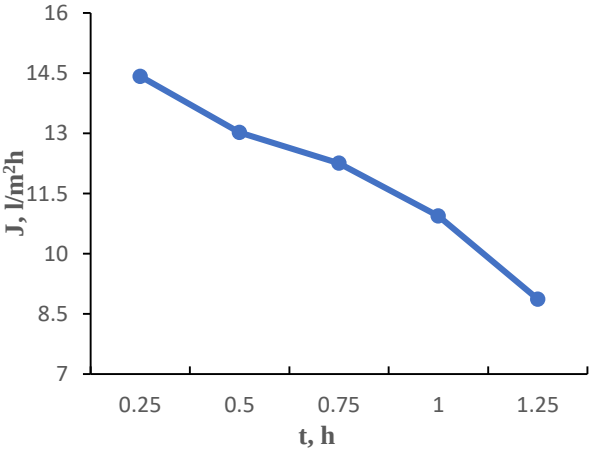

Fig. 4. Permeate flux declined over time for UF PVDF membrane at Co=65 NTU, T=25°C, and QF=20 L/h

4.2. Water turbidity

Even though the Tigris River water, is the primary source of drinking water in Baghdad, which contains a high concentration of TSS, the implementation of MF, and UF processes effectively eliminates these solids. Consequently, the water's turbidity is consistently below 1 NTU. As shown in Fig. 5 the turbidity values after 1.25 hours of treatment were 2.7 NTU for the P.P. MF membrane, 0.86 NTU for the ceramic MF membrane, and 0.38 NTU for the PVDF UF membrane. Higher turbidity levels contribute to an increased accumulation rate of solids, pore-clogging, and hydraulic resistance, which in turn lowers removal efficiency, and vice versa. The highest removal efficiencies achieved were 98.7% for the PVDF UF membrane, followed by 97.13% for the ceramic MF membrane, and 91% for the P.P. MF membrane, as shown in Fig. 6. These results align with the findings of Islam et al, [39].

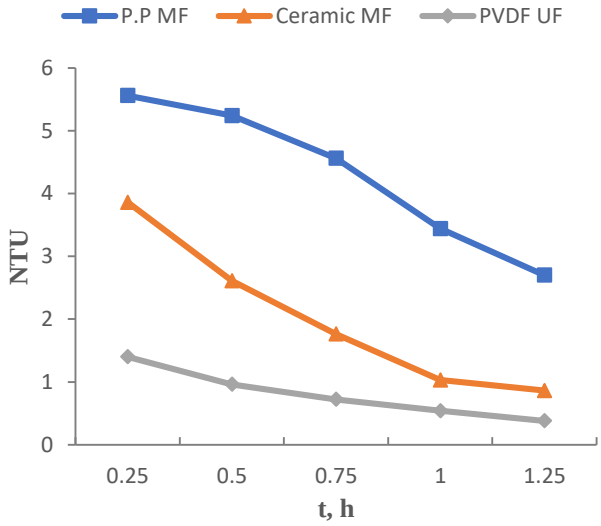

Fig. 5. Effect of Removal turbidity with time for different membranes at Co=65 NTU, T=25°C, QF=20 L/h

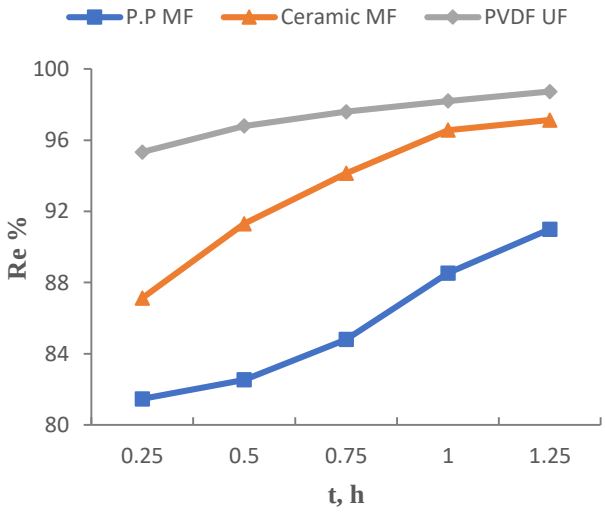

Fig. 6. Effect of time on turbidity removal efficiency for different membranes at Co=65 NTU, T=25°C, QF=20 L/h

4.3. Total suspended solid

Total Suspended Solids measure the concentration of insoluble materials in water, including organic (detritus and biosolids) and inorganic (sand and fine colloids) constituents. Although the World Health Organization has not set a limit for TSS, the European Union has established a maximum level of 25 mg/L [7]. After filtration, TSS values reached 10 mg/L for the P.P. MF membrane, achieving a 75% removal efficiency; 7 mg/L for the ceramic MF membrane, with 83% removal efficiency; and 5 mg/L for the PVDF UF membrane, with 88% removal efficiency, as shown in Fig. 7. These levels fall within permissible limits. These results are consistent with Mansoor, and Al Hassany et al, [40, 41], with the current study demonstrating significantly improved TSS reductions compared to previous studies.

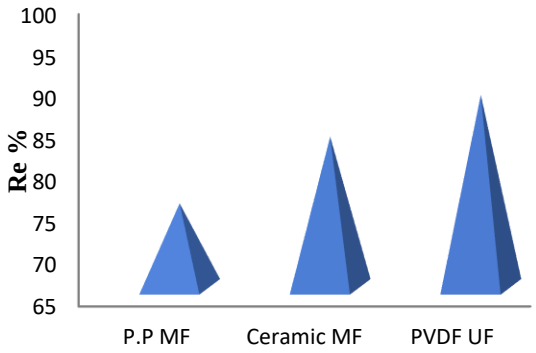

Fig. 7. The total suspended solid TSS removal efficiency for MF and UF membranes at Co=65 NTU, T=25°C, flowrate QF=20 L/h

4.6. Bacteriological analyses

The World Health Organization recommends that the permissible limit for Total Coliform in water should be less than 1.8 MPN/100 ml. Additionally, acceptable levels of E. coli are crucial for indicating good water quality. In the Tigris River, E. coli and Total Coliform levels were found to be 1700 MPN/100 mL and 2200 MPN/100 mL, respectively. These high concentrations indicate contamination of the river water with sewage, either directly or indirectly, posing a threat to public health and environmental quality due to the elevated bacterial load, which negatively affects aquatic life.

After applying the membrane filtration process, the results revealed that the Total Coliform count was reduced to 23 MPN/100 mL, achieving an excellent removal efficiency of 98.8% for the P.P. MF membrane and 9.2 MPN/100 mL with an efficiency of 99.5% for the ceramic MF membrane. The PVDF UF membrane demonstrated an even greater efficacy, reducing Total Coliform to 2.2 MPN/100 mL with a 99.9% removal efficiency. While these percentages reflect significant reductions, they remain slightly above the WHO's permissible limit of zero MPN/100 mL, likely due to leaks from sewage and solid waste disposal systems. Therefore, additional treatment stages may be necessary to achieve compliance with these limits.

In the case of E. Coli bacteria, after treatment with the P.P MF membrane, the count was 23/100 ml with an efficiency of 98.6%. For the ceramic MF and PVDF UF membranes, the count was 0 MPN/100 ml with an efficiency of 100%. These results fall within the permissible limits set by the World Health Organization, as shown in Fig. 8. This study agreed with Ghafil, et al [42].

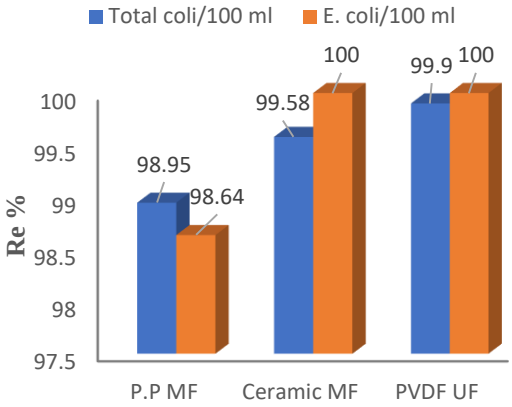

Fig. 8. The removal efficiency of bacteria using micro and ultrafiltration membranes at Co=65 NTU, T=25°C, F=20 L/h

Table 3 summarizes the results of the Tigris River water's physical, chemical, and biological properties in Baghdad during April 2024.

Table 3. Physical, chemical, and biological characteristics of the Tigris River in Baghdad during April month /2024 at Co=65 NTU, T=25°C, F=20 L/h

Parameter	WHO standard [43]	Permeate of P.P MF 1 µm	Permeate of ceramic MF 0.5 µm	Permeate of PVDF UF 500KD
Temperature °C	-	25 ±1°C	25 ±1°C	25 ±1°C
PH	6.5-8.5	7.88	7.9	7.85
E.C us/cm	1000	581	575	564
TDS mg/l	1000	280	277	271
TSS mg/l	25	10	7	5
Turbidity NTU	5	2.7	0.86	0.38
M.P.N of Total coliform /100 ml	<1.8	23	9.2	2.2
M.P. N of E. coli /100 ml	Zero	23	Zero	Zero

4.4. Theoretical results of filtration models

The Hermia model was used to analyze the filtration process in crossflow membrane filtration for Tigris River water. Hermia's models were applied to a ceramic membrane with a pore size of 0.5 microns, selected to represent the microfiltration technique. In contrast, a polyvinylidene fluoride (PVDF) membrane with a molecular weight cut-off of 500 kDa was chosen to represent the ultrafiltration technique. In most cases, the models show reasonable agreement with experimental data, displaying linear correlations.

The estimated flux of ceramic MF membrane is as follows: 346.71, 351.76, 358.20, and 378.42 l/m^{2}h for the complete pore blocking, standard pore blocking, intermediate pore blocking, and cake filtration models, respectively. These results show that the cake filtration model was the most effective in describing the fouling of the ceramic MF membrane, with a high R^2 value of 0.992. Additionally, the intermediate pore-blocking model closely matched the experimental permeation flux data, with an R2 value of 0.98, except at the initial stages of operation as shown in Fig. 9 to Fig. 12**,** therefore, it can be concluded that the cake formation model, followed by the intermediate pore-blocking model, provided the most accurate predictions under the tested operational conditions. This behavior is consistent with Poerio et al, and Sadek et al, [44, 45].

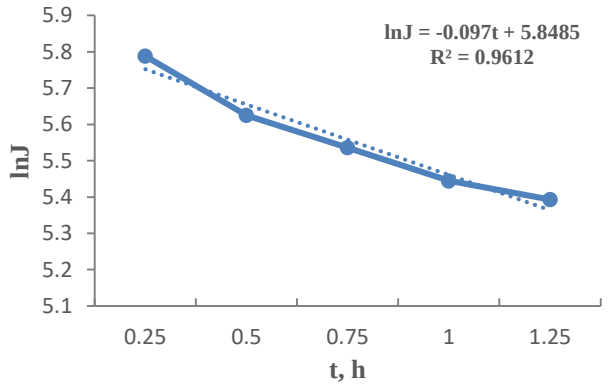

Fig. 9. Complete pore-blocking model of ceramic MF membrane at Co=30 NTU, T=25°C, QF=20 L/h

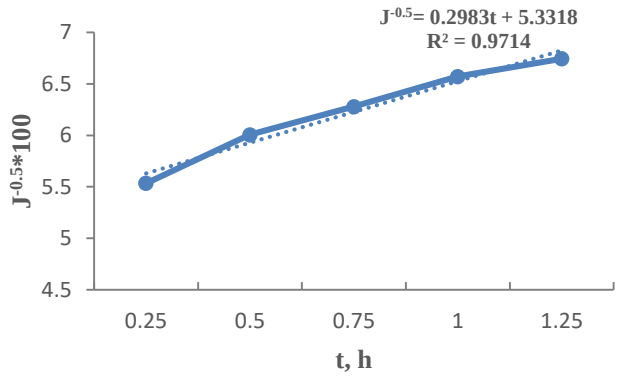

Fig. 10. Standard pore blocking model of ceramic MF membrane at Co=30 NTU, T=25°C, QF=20 L/h

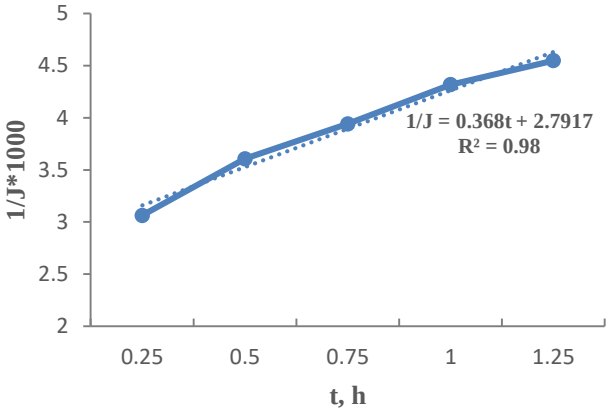

Fig. 11. Intermediate pore blocking model of ceramic MF membrane at Co=30 NTU, T=25°C, QF=20 L/h

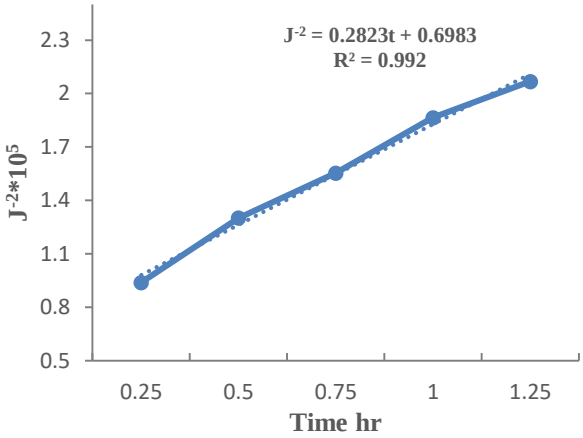

Fig. 12. Cake filtration model of ceramic MF membrane at Co=30 NTU, T=25°C, QF=20 L/h

On the other hand, the estimated flux values for the PVDF ultrafiltration membrane are as follows: 16.56, 17.09, 17.86, and 21.27 L/m²h for the complete pore blocking, standard pore blocking, intermediate pore blocking, and cake filtration models, respectively. There are no significant differences between the experimental data and the model predictions. Among the fouling models, the complete pore-blocking model provided the best fit for the PVDF UF membranes, with an R^2 value of 0.949, indicating a strong correlation with the experimental data. These results suggest that the particles are similar in size to the average pore size. As particles clog individual pores, the flow is redirected to adjacent pores, leading to their subsequent clogging. This phenomenon reduces the available membrane area and increases membrane resistance. Additionally, the standard pore-blocking model also showed a good correlation with the experimental permeation flux data, achieving an R^2 value of 0.9326, as shown in Fig. 13 to Fig. 16. This behavior is consistent with Zhang et al, and Garcia-Castello et al, [46, 47].

In PVDF membranes, the dominant mechanism of fouling is the complete pore-blocking model, primarily due to their small pore size, which causes immediate

clogging by fine particles. This is followed by the standard pore-blocking model, where some particles are partially deposited within the pores without completely blocking them. This reflects how the membrane interacts with fine particles through the physical barriers created by the pores. In contrast, ceramic membranes mainly exhibit the cake filtration model, where larger particles accumulate on the surface, forming a dense layer that restricts flow. This is followed by the intermediate pore-blocking model, where some particles penetrate the pores partially before causing complete clogging. The differences in these fouling mechanisms are attributed to variations in pore size and the nature of the contaminants. PVDF membranes are designed to handle smaller particles, while ceramic membranes are better suited for larger particles, resulting in distinct mechanisms for how contaminants interact with each type of membrane.

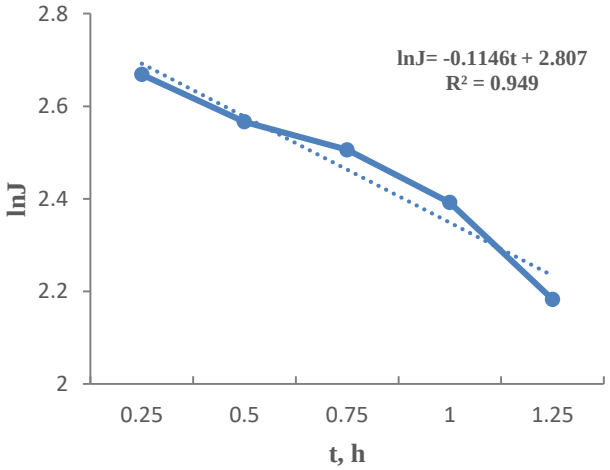

Fig. 13. Complete pore-blocking model of PVDF UF membrane at Co=30 NTU, T=25°C, QF=20 L/h

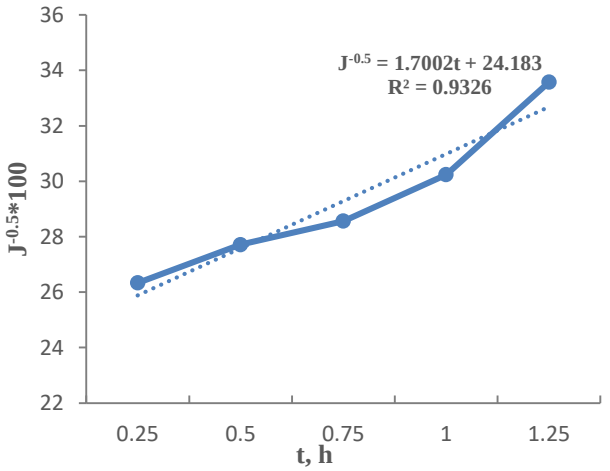

Fig. 14. Standard pore blocking model of PVDF UF membrane at Co=30 NTU, T=25°C, QF=20 L/h

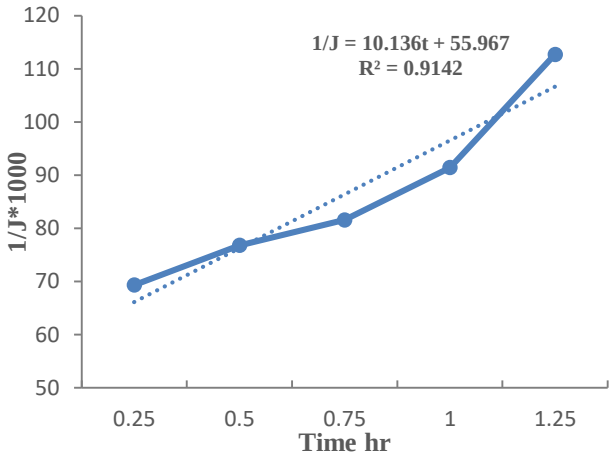

Fig. 15. Intermediate pore blocking model of PVDF UF membrane at Co=30 NTU, T=25°C, QF=20 L/h

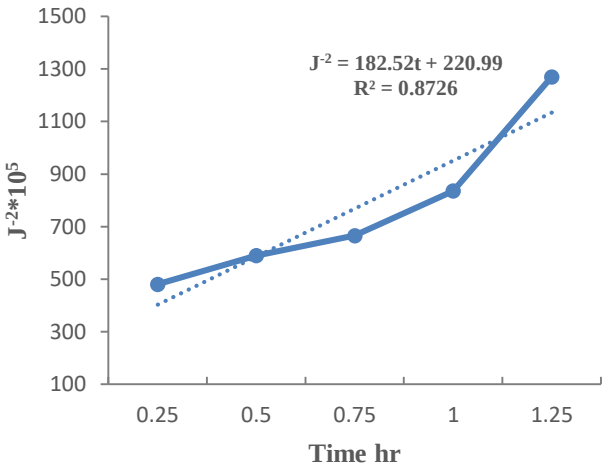

Fig. 16. Cake filtration model of PVDF UF membrane at Co=30 NTU, T=25°C, QF=20 L/h

5- Conclusion

The use of micro and ultra-membrane filtration processes is an efficient technique for removing turbidity, bacteria, and suspended particles from water, making it a promising alternative to traditional water treatment methods. The results indicated that permeate flux decreases over time, with decreasing percentages of 23.11% for polypropylene membranes, 32.63% for ceramic membranes, and 38.48% for PVDF membranes. In terms of removal efficiency, the highest value was achieved using the PVDF UF membrane at 98.7%, followed by the ceramic MF membrane at 97.13%, and the PP MF membrane at 91%. Regarding total suspended solids, the PP MF membrane achieved a 75% removal efficiency. The ceramic MF membrane showed a removal efficiency of 83%, while the PVDF UF membrane achieved the highest removal efficiency at 88%.

Additionally, the removal efficiency of E. coli was notable, with the PP MF membrane achieving 98.8%, the ceramic MF membrane reaching 99.5%, and the PVDF UF membrane delivering the highest performance with a 99.9% removal efficiency. Hermia model provided an

accurate prediction of fouling behavior over time for each membrane, aiding in understanding the mechanisms of membrane fouling and identifying the dominant fouling type. The results revealed that the cake filtration model was the most suitable for describing the fouling of the ceramic MF membrane, with a high R^2 value of 0.992. For the PVDF UF membrane, the complete pore-blocking model was found to be the most effective, with an R^2 value of 0.949. These findings highlight the importance of selecting the appropriate fouling model for optimizing membrane performance. These membranes can be relied upon as one of the modern solutions that contribute to achieving the required water quality standards more effectively, making them an attractive option for entities concerned with improving water quality.

Nomenclature

Symbol	Description	Units
μ	Viscosity	kg/m.sec
A	Area	m2
C_F	Feed Concentration	mg/l
C_P	Permeate Concentration	mg/l
J	Permeation Flux	m^3/m^2.sec
J_0	Initial Permeate Flux	m^3/m^2.sec
K_b	Mass Transfer Coefficient for Complete Pore Blocking Model	m/sec
K_c	Mass Transfer Coefficient for Cake Filtration Model	m/sec
K_i	Mass Transfer Coefficient for Intermediate Pore Blocking Model	m/sec
K_s	Mass Transfer Coefficient for Standard Pore Blocking Model	m/sec
Q_{feed}	Feed Flow Rate	l/h
$Q_{permeate}$	Permeate (or Product) Flow Rate	l/h
Re %	Removal efficiency	
R^2	Correlation of Coefficient	
R_c	Cake Resistance	m-1
R_m	Clean Membrane Resistance	m-1
R_p	Pore Blocking Resistance	m-1
t	Time	h
T	Temperature	°C
P	Pressure	Bar

Abbreviation

Symbol	Description
MF	Microfiltration
UF	Ultrafiltration
P.P	Polypropylene membrane
PVDF	Polyvinyl dene fluoride
TDS	Total dissolved solids
TSS	Total suspended solids
E.C	Electrical conductivity
TMP	Transmembrane pressure
WHO	World health organizations

Reference

[1] P. K. Singh *et al.*, "Critical review on toxic contaminants in surface water ecosystem: sources, monitoring, and its impact on human health," *Environmental Science and Pollution Research.*, pp. 1–35, 2024. https://doi.org/10.1007/s11356-024-34932-0

[2] S. Giri, "Water quality perspective in Twenty First Century: Status of water quality in major river basins, contemporary strategies and impediments: A review," *Applied Sciences.*, vol. 271, p. 116332, 2021. https://doi.org/10.3390/app11093743

[3] N. Rahmanian *et al.*, "Analysis of physiochemical parameters to evaluate the drinking water quality in the State of Perak, Malaysia," *Jornal of. Chemistry.*, vol. 2015, no. 1, p. 716125, 2015. https://doi.org/10.1155/2015/716125

[4] F. C. Bull *et al.*, "World Health Organization 2020 guidelines on physical activity and sedentary behaviour," *British Journal of sports medicine.*, vol. 54, no. 24, pp. 1451–1462, 2020, https://doi.org/10.1136/bjsports-2020-102955

[5] L. Kumar, R. Kumari, A. Kumar, I. A. Tunio, and C. Sassanelli, "Water quality assessment and monitoring in Pakistan: A comprehensive review," *Sustainability*, vol. 15, no. 7, p. 6246, 2023, https://doi.org/10.3390/su15076246

[6] N. Al-Ansari, N. Adamo, V. Sissakian, S. Knutsson, and J. Laue, "Water resources of the Tigris River catchment," *Journal of Earth Sciences and Geotechnical Engineering.*, vol. 8, no. 3, pp. 21–42, 2018.

[7] D. V Chapman, *Water quality assessments: a guide to the use of biota, sediments and water in environmental monitoring*. CRC Press, 2021, https://doi.org/10.1201/9781003062103

[8] G. Basílico, L. de Cabo, and A. Faggi, "Phytoremediation of water and wastewater: on-site and full-scale applications," *Phytoremediation: Management of Environmental Contaminants, Volume 2. Vol. 2*, pp. 51–60, 2015. https://doi.org/10.1007/978-3-319-10969-5_5

[9] J. Hoslett *et al.*, "Surface water filtration using granular media and membranes: A review," *Science of the Total Environment*, 639, pp. 1268–1282, 2018, https://doi.org/10.1016/j.scitotenv.2018.05.247

[10] A. Bardhan, A. Akhtar, and S. Subbiah, "Microfiltration and ultrafiltration membrane technologies," in *Advancement in Polymer-Based Membranes for Water Remediation*, Elsevier, 2022, pp. 3–42, https://doi.org/10.1016/B978-0-323-88514-0.00001-2

[11] E. Nascimben Santos, Z. László, C. Hodúr, G. Arthanareeswaran, and G. Veréb, "Photocatalytic membrane filtration and its advantages over conventional approaches in the treatment of oily wastewater: *Asia-Pacific Journal of Chemical Engineering.*, vol. 15, no. 5, p. e2533, 2020, https://doi.org/10.1002/apj.2533

[12] E. Obotey Ezugbe and S. Rathilal, "Membrane technologies in wastewater treatment: a review," *Membranes (Basel).*, vol. 10, no. 5, p. 89, 2020, https://doi.org/10.3390/membranes10050089

[13] M. Bodzek and K. Konieczny, "The use of ultrafiltration membranes made of various polymers in the treatment of oil-emulsion wastewaters," *Waste management.*, vol. 12, no. 1, pp. 75–84, 1992, https://doi.org/10.1016/0956-053X(92)90011-7

[14] S. P. Bera, M. Godhaniya, and C. Kothari, "Emerging and advanced membrane technology for wastewater treatment: A review," *Journal of Basic Microbiology.*, vol. 62, no. 3–4, pp. 245–259, 2022, https://doi.org/10.1002/jobm.202100259

[15] K. Elsaid, M. Kamil, E. T. Sayed, M. A. Abdelkareem, T. Wilberforce, and A. Olabi, "Environmental impact of desalination technologies: A review," *Science of the total environment.*, vol. 748, p. 141528, 2020, https://doi.org/10.1016/j.scitotenv.2020.141528

[16] V. Srivastava, S. K. Mishra, U. P. Singh, R. Kumar, L. Sexana, and R. Kumar, "Membranes, Membranes Phenomena and Applications-A Review," *IJRAR-International Journal of Research and Analytical Reviews (IJRAR).*, vol. 9, no. 3, pp. 403–467, 2022.

[17] A. Nqombolo, A. Mpupa, R. M. Moutloali, and P. N. Nomngongo, "Wastewater treatment using membrane technology," *Wastewater and water quality.*, vol. 29, pp. 30–40, 2018.

[18] M. K. Purkait, M. K. Sinha, P. Mondal, and R. Singh, "Introduction to membranes," in *Interface science and technology*, vol. 25, Elsevier, 2018, pp. 1–37, https://doi.org/10.1016/B978-0-12-813961-5.00001-2

[19] S. M. Samaei, S. Gato-Trinidad, and A. Altaee, "The application of pressure-driven ceramic membrane technology for the treatment of industrial wastewaters–A review," *Separation and Purification Technology.*, vol. 200, pp. 198–220, 2018, https://doi.org/10.1016/j.seppur.2018.02.041

[20] M. W. Hakami, A. Alkhudhiri, S. Al-Batty, M.-P. Zacharof, J. Maddy, and N. Hilal, "Ceramic microfiltration membranes in wastewater treatment: filtration behavior, fouling and prevention," *Membranes (Basel).*, vol. 10, no. 9, p. 248, 2020, https://doi.org/10.3390/membranes10090248

[21] H. Xiang, X. Min, C.-J. Tang, M. Sillanpää, and F. Zhao, "Recent advances in membrane filtration for heavy metal removal from wastewater: A mini review," *Journal of Water Process Engineering.*, vol. 49, p. 103023, 2022, https://doi.org/10.1016/j.jwpe.2022.103023

[22] K. Castro and R. Abejón, "Removal of Heavy Metals from Wastewaters and Other Aqueous Streams by Pressure-Driven Membrane Technologies: An Outlook on Reverse Osmosis, Nanofiltration, Ultrafiltration and Microfiltration Potential from a Bibliometric Analysis," *Membranes (Basel).*, vol. 14, no. 8, p. 180, 2024, https://doi.org/10.3390/membranes14080180

[23] C. Yin-ru, L. Yu-jen, and L. Duu-jong, "Membrane fouling during water or wastewater treatments: Current research updated," *Journal of the Taiwan Institute of Chemical Engineers*, vol. 0, pp. 1–9, 2019, https://doi.org/10.1016/j.jtice.2017.12.019

[24] M. H. Salih, A. F. Al-Alawy, "A novel forward osmosis for treatment of high-salinity East Baghdad oilfield produced water as a part of a zero liquid discharge system", Desalination and Water Treatment, Vol. 248, pp. 18-27, 2022, https://doi.org/10.5004/dwt.2022.28070

[25] F. Ahmed, B. S. Lalia, V. Kochkodan, N. Hilal, and R. Hashaikeh, "Electrically conductive polymeric membranes for fouling prevention and detection: A review," *Desalination*, vol. 391, pp. 1–15, 2016, https://doi.org/10.1016/j.desal.2016.01.030

[26] M. Al-Shaeli, S. J. D. Smith, E. Shamsaei, H. Wang, K. Zhang, and B. P. Ladewig, "Highly fouling-resistant brominated poly (phenylene oxide) membranes using surface grafted diethylenetriamine," *RSC advances.*, vol. 7, no. 59, pp. 37324–37330, 2017, https://doi.org/10.1039/C7RA05524B

[27] S. Laohaprapanon, A. D. Vanderlipe, B. T. Doma Jr, and S.-J. You, "Self-cleaning and antifouling properties of plasma-grafted poly (vinylidene fluoride) membrane coated with ZnO for water treatment," *Journal of the Taiwan Institute of Chemical Engineers.*, vol. 70, pp. 15–22, 2017, https://doi.org/10.1016/j.jtice.2016.10.019

[28] P. C. Y. Wong, Y.-N. Kwon, and C. S. Criddle, "Use of atomic force microscopy and fractal geometry to characterize the roughness of nano-, micro-, and ultrafiltration membranes," *Journal of Membrane Science.*, vol. 340, no. 1–2, pp. 117–132, 2009, https://doi.org/10.1016/j.memsci.2009.05.018

[29] H. Xu *et al.*, "Outlining the roles of membrane-foulant and foulant-foulant interactions in organic fouling during microfiltration and ultrafiltration: A mini-review," *Frontiers in chemistry*, vol. 8, p. 417, 2020, https://doi.org/10.3389/fchem.2020.00417

[30] I. A. Khan, Y.-S. Lee, and J.-O. Kim, "A comparison of variations in blocking mechanisms of membrane-fouling models for estimating flux during water treatment," *Chemosphere*, vol. 259, p. 127328, 2020, https://doi.org/10.1016/j.chemosphere.2020.127328

[31] S. Hube, J. Wang, L. N. Sim, T. H. Chong, and B. Wu, "Direct membrane filtration of municipal wastewater: Linking periodical physical cleaning with fouling mechanisms," *Separation and Purification Technology.*, vol. 259, p. 118125, 2021, https://doi.org/10.1016/j.seppur.2020.118125

[32] H. Choi, K. Zhang, D. D. Dionysiou, D. B. Oerther, and G. A. Sorial, "Effect of permeate flux and tangential flow on membrane fouling for wastewater treatment," *Separation and Purification Technology.*, vol. 45, no. 1, pp. 68–78, 2005, https://doi.org/10.1016/j.seppur.2005.02.010

[33] R. Bai and H. F. Leow, "Modeling and experimental study of microfiltration using a composite module," *Journal of membrane science.*, vol. 204, no. 1–2, pp. 359–377, 2002, https://doi.org/10.1016/S0376-7388(02)00063-7

[34] C.-W. Jung, H.-J. Son, and L.-S. Kang, "Effects of membrane material and pretreatment coagulation on membrane fouling: fouling mechanism and NOM removal," *Desalination*, vol. 197, no. 1–3, pp. 154–164, 2006, https://doi.org/10.1016/j.desal.2005.12.022

[35] B. K. Nandi, A. Moparthi, R. Uppaluri, and M. K. Purkait, "Treatment of oily wastewater using low cost ceramic membrane: Comparative assessment of pore blocking and artificial neural network models," *Chemical Engineering Research and Design.*, vol. 88, no. 7, pp. 881–892, 2010, https://doi.org/10.1016/j.cherd.2009.12.005

[36] K. Konieczny and J. Rafa, "Modeling of the membrane filtration process of natural waters," *Polish Journal of Environmental Studies.*, vol. 9, no. 1, pp. 57–64, 2000.

[37] A. Gul, J. Hruza, and F. Yalcinkaya, "Fouling and Chemical Cleaning of Microfiltration Membranes: A Mini-Review". *Polymers* 2021, 13, 846, https://doi.org/10.3390/polym13060846

[38] M. H. Salih, A. M. Al-Yaqoobi, H. A. Hassan, and A. F. Al-Alawy, "Assessment of the Pressure Driven Membrane for the Potential Removal of Aniline from Wastewater.," *Jornal of Ecological Engineering.*, vol. 24, no. 8, 2023. https://doi.org/10.12911/22998993/166283

[39] G. A. AL-Dulaimi and M. K. Younes, "Assessment of potable water quality in Baghdad City, Iraq," *Air, Soil and Water Research.*, vol. 10, p. 1178622117733441, 2017, https://doi.org/10.1177/1178622117733441

[40] P. Mac Berthouex and L. C. Brown, *[45] M. K. Mensoor, "Monitoring Pollution of the Tigris River in Baghdad by Studying Physico-Chemical Characteristics," 2021.* CRC Press, 2017, https://doi.org/10.21203/rs.3.rs-1074093/v1

[41] J. S. Al Hassany and H. E. Al Bayaty, "Screening of epiphytic algae on the aquatic plant Phragmites australis inhabiting Tigris river in Al-Jadria site, Baghdad, Iraq," *Baghdad science journal.*, vol. 14, no. 1, p. 85, 2017, http://dx.doi.org/10.21123/bsj.2017.14.1.0085

[42] J. A. Ghafil, H. K. Zghair, and A. K. Zgair, "Chemical and microbiological properties of drinking water in the city of Baghdad," *Diyala Journal of Medicine*, 2022. https://doi.org/10.26505/djm.v23i1.924

[43] F. Edition, "Guidelines for drinking-water quality," WHO chronicle., vol. 38, no. 4, pp. 104–108, 2011.

[44] T. Poerio *et al.*, "Identification of fouling mechanisms in cross-flow microfiltration of olive-mills wastewater," *Journal of Water Process Engineering.*, vol. 49, p. 103058, 2022, https://doi.org/10.1016/j.jwpe.2022.103058

[45] S. A. Sadek, S. M. Al-Jubouri, and S. Al-Batty, "Investigating the Fouling Models of the Microfiltration Mixed Matrix Membranes-Based Oxide Nanoparticles Applied for Oil-in-Water Emulsion Separation," *Iraqi Journal of Chemical and Petroleum Engineering.*, vol. 25, no. 2, pp. 1–16, 2024. https://doi.org/10.31699/IJCPE.2024.2.1

[46] W. Zhang, W. Liang, G. Huang, J. Wei, L. Ding, and M. Y. Jaffrin, "Studies of membrane fouling mechanisms involved in the micellar-enhanced ultrafiltration using blocking models," *RSC Advances.*, vol. 5, no. 60, pp. 48484–48491, 2015, https://doi.org/10.1039/C5RA06063J

[47] E. M. Garcia-Castello, A. D. Rodriguez-Lopez, S. Barredo-Damas, A. Iborra-Clar, J. Pascual-Garrido, and M. I. Iborra-Clar, "Fabrication and performance of low-fouling UF membranes for the treatment of isolated soy protein solutions," *Sustainability*, vol. 13, no. 24, p. 13682, 2021, https://doi.org/10.3390/su132413682

تقييم أغشية الترشيح الدقيق والفائق لتحسين جودة المياه: إزالة العكارة، المواد الصلبة العالقة، والبكتيريا من نهر دجلة

نور جاسم التميمي [١،*]، احمد فائق العلوي [١]، مؤيد الشعيلي [٢]

١ قسم الهندسة الكيمياوية، كلية الهندسة، جامعة بغداد، بغداد، العراق
٢ كلية العلوم والتكنولوجيا والطب، جامعة لوكسمبورغ، لوكسمبورغ

الخلاصة

يتعرض نهر دجلة في بغداد للتلوث بشكل متزايد بسبب الأنشطة الصناعية والزراعية ومياه الصرف الصحي غير المعالجة، مما يشكل مخاطر جسيمة على الصحة العامة والبيئة. ويؤدي هذا التلوث إلى تدهور جودة المياه من خلال العديد من الملوثات الفيزيائية والكيميائية والبيولوجية. يهدف هذا البحث إلى استخدام تقنيات الترشيح الغشائي لمعالجة مياه نهر دجلة، وتحسين جودة المياه وضمان إمدادات مياه نظيفة وآمنة. تقيم الدراسة كفاءة أغشية الترشيح الفائق المصنوعة من البولي بروبلين 1 (P.P) ميكرومتر، والترشيح الدقيق الخزفي ٠,٥ ميكرومتر، وأغشية الترشيح الفائق المصنوعة من البولي فينيلدين فلوريد 500KD (PVDF) في إزالة العكارة والمواد الصلبة العالقة الكلية(TSS) ، والإشريكية القولونية، وتأثيرها على تدفق النفاذية. أجريت التجارب عند درجة حرارة ٢٥ درجة مئوية ومعدل تدفق ٢٠ لتر/ساعة، مع فترات منتظمة وعكارة أولية تبلغ ٦٥ وحدة حرارية بريطانية. أشارت النتائج إلى أنه بعد ١,٢٥ ساعة من التشغيل، انخفض تدفق النفاذية بنسبة ٢٣,١٢٪ لأغشية البولي بروبيلين، و ٣٢,٦٣٪ للأغشية الخزفية، و ٣٨,٤٨٪ لأغشية .PVDF أظهر غشاء PVDF أفضل أداء، حيث أزال ٩٨,٧٪ من العكارة، و ٨٨٪ من إجمالي المواد الصلبة العالقة(TSS) ، و ١٠٠٪ من الإشريكية القولونية. هذا يجعله الغشاء الأكثر كفاءة بين الخيارات المختبرة. تم استخدام نموذج هيرميا لدراسة التلوث في أغشية الترشيح الفائق (UF) والترشيح الدقيق .(MF) أظهرت النتائج أن تكوين الكعكة ونماذج حجب المسام القياسية هي أفضل من توقع سلوك التدفق للغشاء الخزفي، في حين كانت نماذج حجب المسام الكاملة والمتوسطة أكثر فعالية لغشاء .PVDF تُظهر هذه الدراسة أن الترشيح الغشائي يحسن جودة مياه نهر دجلة من خلال إزالة العكارة والمواد الصلبة العالقة والبكتيريا، مما يضمن إمدادات مياه آمنة.

الكلمات الدالة: الترشيح الدقيق، الترشيح الفائق، نهر دجلة، نموذج هيرميا، تلوث الأغشية.